

In Table IV we have collected the calculated 3-21G, 6-31G**/3-21G, and MP2/6-31G**/3-21G energies of TSs 20-23. Up to the first two levels, the energy differences between the transition structures do not differ sensibly from what expected on the basis of the 3-21G//MNDO data (see Table II). However, inclusion of electron correlation effects by second-order Møller-Plesset correction shows that type 3 and type 4 TS (both including an *s*-trans configured aldehyde moiety) are much more stable than those calculated by 3-21G//MNDO. Since type 3 TS implies the opposite topicity compared to type 1 TS, this has a major implication on the stereochemical outcome of the reaction. In particular the critical dependence of the selectivity on the bulk of the enone carbonyl substituent R³ could be explained by the well-known ground-state correlation in conjugated ketones between the size of R³ and the relative population of the *s*-cis and *s*-trans conformations of the enone.²⁴ An increase in the bulk of R³ has the effect of destabilizing the *s*-trans conformation by allylic strain, and therefore it increases the relative population of the *s*-cis conformer. If this feature is carried over to the TS, this should rule out a contribution by type 3 and type 4 geometry when R³ is large. The stereochemical outcome would therefore depend only on the energy difference between type 1 and type 2 TSs, which are well separated at all computational levels. The effect of the

(24) Oelichmann, H.-J.; Bougeard, D.; Schrader, B. *Angew. Chem., Int. Ed. Engl.* 1985, 1404.

enolate substituent R¹ is much less clear-cut and a detailed analysis of it must await for a higher level of theory calculation of substituted transition structures.

Conclusion

In conclusion, we have shown that four different cyclic, eight-membered transition structures can be located for the conjugate addition of acetaldehyde lithium enolate to acrolein. Their geometrical features and relative energies are similar at the 3-21G//MNDO or the HF/3-21G level.

Their relative stability has been evaluated up to the MP2/6-31G**/3-21G level and can qualitatively account for the experimentally observed stereoselectivity in the Michael addition reactions of ketone and ester enolates. These calculations support the mechanistic rationale invoked by several authors¹ in order to account for the stereochemical outcome of this reaction.

Acknowledgment. This work was supported by the Commission of the European Communities [Grant SC1*.0324.C(JR)], MURST (Rome), and CNR (Rome). We thank Glaxo-Verona for a research fellowship to A. M.C. The Gaussian 88 calculations were performed on the Convex-C220 at the Centro Interuniversitario Lombardo Elaborazione Automatica (CILEA).

Supplementary Material Available: Energies and Cartesian coordinates of structures 4-23 (9 pages). This material is contained in many libraries on microfiche, immediately follows this article in the microfilm version of the journal, and can be ordered from the ACS; see any current masthead page for ordering information.

Anomeric and Reverse Anomeric Effects in the Gas Phase and Aqueous Solution

Christopher J. Cramer

Department of Chemistry, University of Minnesota, 207 Pleasant Street SE, Minneapolis, Minnesota 55455

Received September 21, 1992

Anomeric stabilization within the (hydroxymethyl)oxonium, (hydroxymethyl)ammonium, and 2-tetrahydropyranosylammonium systems has been explored at both the ab initio (MP2/6-31G**//HF/6-31G**) and semiempirical (AM1) levels of theory. Aqueous solvation effects have been explored using a continuum dielectric model including local field and hydrophobic/hydrophilic effects (AM1-SM2). By analysis of C-O bond rotational coordinates in (hydroxymethyl)oxonium and stationary points for the other two molecules, it is apparent that hyperconjugative delocalization is operative in all instances of favorable orbital overlap; i.e., an anomeric effect exists. It is smaller in the ammonium case by comparison to the oxonium. Aqueous solvation tends to reduce anomeric stabilization, especially for the tetrahydropyranosyl system, where steric and dipole-dipole effects are also in opposition. The combination of these effects is sufficient to outweigh anomeric stabilization and leads to an equilibrium dominated by the equatorially substituted isomer, i.e., the reverse anomeric effect. Implications for the relative basicity of axial and equatorial anomeric substituents are also discussed.

Introduction

Electronegative substituents at C(2) of a pyranose ring (C(1) in sugar notation) have a tendency to prefer axial orientations over equatorial in spite of steric influences which would otherwise favor the converse. This phenomenon, recognized now for nearly a century, has been termed the anomeric effect.¹ It has more recently been gener-

alized to state that in a molecular fragment W-X-Y-Z, where Z is an electron-withdrawing group, X possesses one or more lone pairs, and W and Y are of intermediate electronegativity, the synclinal (*gauche*) arrangement of atoms is preferred over the antiperiplanar (*trans*).²

Historically, in order to account for this apparent energetic anomaly in pyranose rings, interpretations based

(1) (a) Jungins, C. L. *Z. Phys. Chem.* 1905, 52, 97. (b) Lemieux, R. U. In *Molecular Rearrangements*, de Mayo, P., Ed.; Interscience: New York, 1964. (c) *Anomeric Effect, Origin and Consequences*; Szarek, W. A.; Horton, D., Eds.; ACS Symposium Series 87; American Chemical Society: Washington, DC, 1979. (d) Kirby, A. J. *The Anomeric Effect and Related Stereoelectronic Effects at Oxygen*; Springer-Verlag: New York, 1983. (e) Deslongchamps, P. *Stereoelectronic Effects in Organic Chemistry*; Pergamon: New York, 1983.

(2) (a) de Wolf, N.; Romers, C.; Altona, C. *Acta Crystallogr.* 1967, 22, 715. (b) de Hoog, A. J.; Buys, H. R.; Altona, C.; Havinga, E. *Tetrahedron* 1969, 25, 3365. (c) Lemieux, R. U. *Pure Appl. Chem.* 1971, 25, 527. (d) Eliel, E. L.; Bailey, W. F. *J. Am. Chem. Soc.* 1974, 96, 1798. (e) Schleyer, P. v. R.; Jemmis, E. D.; Spitznagel, G. W. *Ibid.* 1975, 107, 6393. (f) Reed, A. E.; Schleyer, P. v. R. *Ibid.* 1987, 109, 7362. (g) Denmark, S. E.; Cramer, C. J. *J. Org. Chem.* 1990, 55, 1806. (h) Cramer, C. J. *J. Am. Chem. Soc.* 1990, 112, 7965.

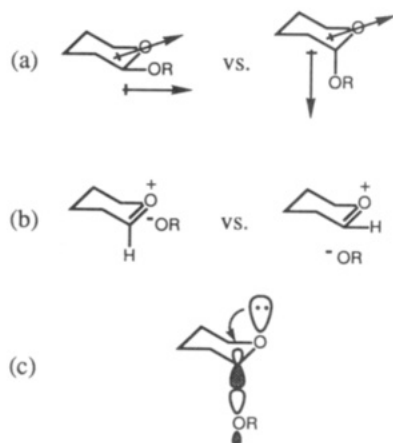


Figure 1. (a) Illustration of the more favorable arrangement of dipoles in the axial 2-alkoxytetrahydropyranoside. (b) Comparison of double bond–no bond resonance structures. (c) Hyperconjugative $n \rightarrow \sigma^*$ interaction which stabilizes the axial isomer.

on dipole–dipole and Coulombic effects between the substituent group and the ring oxygen atom were first proposed (Figure 1).³ However, these models fell out of favor because of their inability to accurately predict experimental syn–anti ratios.⁴ Moreover, they failed to account for significant geometrical changes in substituted pyranosides, which began to appear in numerous X-ray crystallographic studies.^{2a,4,5}

One such change, the lengthening of axial C(2)–X bonds in 2-halopyranosides together with the concomitant shortening of the ring C(2)–O bonds, prompted the invocation of double bond–no bond resonance in these species.⁶ This concept had been successfully applied earlier to the explanation of bond length variations in polyfluoromethanes.⁷ However, this model failed to account for another crystallographic observation, namely the *shortening* of axial C(2)–O_{exo} bonds in 2-oxygenated pyranosides.⁸

In an attempt to reconcile these issues, the newly emerging techniques of computational chemistry began to be applied to this problem.⁹ While they achieved great success in reproducing experimental geometries and energies, interpretation remained a difficult task. Interestingly, each of the two original proposals for the anomeric effect, which might be described as “classical”, generated a quantum mechanical counterpart. Thus, localized molecular orbital (MO) approaches,¹⁰ which focused on total lone pair electron density, were interpreted much like the earlier dipole arguments to give rise to a “gauche effect”.¹¹ However, attempts to rationalize observed geometric changes were still not particularly successful. The alternative approach, which emphasized canonical MO’s,¹² in-

voled perturbational molecular orbital theory¹³ to propose charge transfer from lone-pair orbitals to antibonding C(2)–X σ^* orbitals.^{14,15} This latter explanation has come to be generally accepted and in a comprehensive and elegant paper in 1979, Wolfe, Whangbo, and Mitchell (WWM)¹⁴ finally reconciled the various energetic and geometrical issues associated with the anomeric and exo-anomeric effects (the latter indicating the tendency of the anomeric oxygen *exo* to the ring to *also* prefer a synclinal arrangement, e.g., R–O_{exo}–C(2)–O_{endo} *gauche*).

WWM also noted that, in aminoethanol, there is a large calculated preference for an H–O–C–N arrangement in which significant stabilization arises from delocalization of the *nitrogen* lone pair into the antiperiplanar σ^*_{C-O} orbital.¹⁴ They termed this a *reverse anomeric effect* and suggested that it was further operative in accounting for C(2)–N bond shortening in pyranosyl azides.¹⁶ This was a curious choice of terminology on the part of WWM, since the term *reverse anomeric effect* was in common use at the time as phenomenologically descriptive of the tendency for certain groups to show a preference, which appeared to go beyond sterics, for the equatorial position over the axial (i.e., anti preferred over *gauche*) in 2-substituted pyranosides. In particular, this effect had been established by early NMR studies for both the charged pyridinium group¹⁷ and the neutral carbomethoxy group;¹⁸ both are, in contrast to aminoethanol, notably lacking in available lone pairs on the *exo* substituent.

Such an effect, if general, is far more than a curiosity. Taken out of the ring system, it suggests a preference for anti arrangements of R–O–C–N⁺ groupings where the nitrogen atom is positively charged. At physiological pH, these fragments are found in many biologically important molecules, e.g., aminosugars¹⁹ and clavulanic acid derivatives.²⁰ Moreover, if the anti preference may be extended to R–O–C–O⁺ fragments where the second *oxygen* atom bears a positive charge, it has serious implications for the relative basicities, and hence rates of acidic hydrolysis, of α - and β -glycosides.¹⁷

In an effort to address these issues, and to elucidate to what extent anomeric and reverse anomeric effects occur in such molecular fragments, we have carried out extensive gas-phase calculations on (hydroxymethyl)oxonium and (hydroxymethyl)ammonium at both the semiempirical and *ab initio* levels. We have additionally compared the axial and equatorial isomers of cyclohexylammonium and 2-tetrahydropyranosylammonium in an effort to assess factors unique to the ring systems. Finally, since these protonated molecular fragments exist in predominantly aqueous environments, we have also employed the AM1-SM2 model,²¹ which incorporates a continuum treatment

(3) (a) Edward, J. T. *Chem. Ind. (London)* **1955**, 1107. (b) Anderson, C. B.; Sepp, D. T. *J. Org. Chem.* **1967**, *32*, 607.

(4) Romers, C.; Altona, C.; Buys, H. R.; Havinga, E. *Top. Stereochem.* **1969**, *4*, 39.

(5) Luger, P.; Durette, P. L.; Paulsen, H. *Chem. Ber.* **1974**, *107*, 2615.

(6) Stoddart, J. F. *Stereochemistry of Carbohydrates*, Wiley-Interscience: New York, 1971.

(7) Brockway, L. O. *J. Phys. Chem.* **1937**, *41*, 185.

(8) Berman, H. M.; Chu, S. S. C.; Jeffrey, G. A. *Science* **1967**, *157*, 1576.

(9) (a) Wolfe, S.; Rank, A.; Tel, L. M.; Czismadia, I. G. *J. Chem. Soc. B* **1971**, 136. (b) Jeffrey, G. A.; Pople, J. A.; Radom, L. *Carbohydr. Res.* **1972**, *25*, 117. (c) Tvaroska, I.; Blaha, T. *J. Mol. Struct.* **1975**, *24*, 249.

(d) Gorenstein, D. G.; Findley, J. B.; Luxon, B. A.; Kar, D. *J. Am. Chem. Soc.* **1977**, *99*, 3473.

(10) Wolfe, S.; Tel, L. M.; Haines, W. J.; Robb, M. A.; Czismadia, I. G. *J. Am. Chem. Soc.* **1973**, *95*, 4863.

(11) Wolfe, S. *Acc. Chem. Res.* **1972**, *5*, 102.

(12) David, S.; Eisenstein, O.; Hehre, W. J.; Salem, L.; Hoffman, R. *J. Am. Chem. Soc.* **1973**, *95*, 3806.

(13) Dewar, M. J. S. *The PMO Theory of Organic Chemistry*; Plenum: New York, 1975.

(14) Wolfe, S.; Whangbo, M.-H.; Mitchell, D. J. *Carbohydr. Res.* **1979**, *69*, 1.

(15) To today’s (organic) chemist, the relationship between double bond–no bond resonance and hyperconjugative stabilization is clear, and they are essentially regarded as being different only in notation. At the time of the latter’s proposal, however, this was not at all the case, and the careful counting of resonance structures enjoyed considerable application and interpretation.

(16) (a) Luger, P.; Paulsen, J. *Chem. Ber.* **1974**, *107*, 1579. (b) Paulsen, H.; Gyögydeák, Z.; Friedmann, M. *Ibid.* **1974**, *107*, 1590.

(17) Lemieux, R. U.; Morgan, A. R. *Can. J. Chem.* **1965**, *43*, 2205.

(18) Anderson, C. B.; Sepp, D. T. *J. Org. Chem.* **1968**, *33*, 3272.

(19) Inouye, S. *Chem. Pharm. Bull.* **1968**, *16*, 1134.

(20) (a) Cherry, P. C.; Newall, C. E. In *Chemistry and Biology of Beta-Lactam Antibiotics*; Academic Press: New York, 1982; Vol. 2. (b) Howarth, T. T.; Brown, A. G.; King, T. J. *J. Chem. Soc., Chem. Commun.* **1976**, 266–267. (c) Roberts, M.; Price, B. J. *Medicinal Chemistry, The Role of Organic Chemistry in Drug Research*; Academic: London, 1985.

(21) Cramer, C. J.; Truhlar, D. G. *Science* **1992**, *256*, 213.

of aqueous solvation effects into semiempirical molecular orbital theory.

Computational Methods

All stationary points were fully optimized at the AM1,²² AM1-SM2,²¹ and either the RHF/6-31G** (acyclic systems) or RHF/6-31G* (cyclic systems) levels of theory.²³ All ab initio stationary points were further characterized by analytic frequency calculations. Zero-point vibrational energies (ZPVE) determined therefrom have been scaled by 0.9. Single-point MP2 calculations²⁴ were performed for stationary points at the RMP2/6-31G*(*)//RHF/6-31G*(*) level with core orbitals frozen to substitution. Characterization of rotation coordinates was accomplished by complete geometry optimization at the appropriate level with a single constrained (rotational) degree of freedom. Dihedral angles defined to an oxonium oxygen lone pair are geometrically defined to the plane everywhere equidistant to the two oxonium protons (i.e., bisecting the H-O⁺-H bond angle).

Incorporation of the free energies of solvation for various isomers into relative energies was accomplished in three ways. First, the standard technique of calculating AM1-SM2//AM1-SM2 energies^{21,25a} was employed; this approach necessarily assumes the underlying AM1 heats of formation to be accurate. However, the various SMx solvation models can deliver accurate free energies of solvation even in situations where AM1 does not adequately describe the gas phase molecules; e.g., one can predict accurately the solvation effect on acid-base equilibria (ΔG) even where the gas-phase equilibrium constants (ΔG) are in poor agreement with experiment.^{25b} We therefore also present relative solute energies based on ab initio gas-phase values, i.e., calculated as MP2 or RHF/6-31G**//HF/6-31G** + AM1-SM2//AM1-SM2 - AM1//AM1. Finally, situations arise where structures predicted as stationary points at the ab initio level either do not have counterparts at the AM1 level or the latter are considerably distorted in a geometric sense. In such instances, it is useful to compute the solute energies using the *unrelaxed* gas phase, ab initio geometries, i.e., MP2 or HF/6-31G**//HF/6-31G** + AM1-SM2//HF/6-31G** - AM1//HF/6-31G**. Of the three above methods for assessing the effect of solvation, the second is generally the most reliable and favored slightly over the first—the third is best used only where required.

Ab initio calculations employed the Gaussian 90 suite of programs,²⁶ while the semiempirical calculations used the AMSOL 3.0 package²⁷ which is based on AMPAC 2.1.²⁸

Optimized geometries and energies for all stationary points at the ab initio level are provided as supplementary material.

Results

Although we are particularly interested in cationic acceptor groups, like the oxonium and ammonium ion fragments, it is helpful to first anchor the theory in a system which has already received much theoretical study: dihydroxymethane, **1**. The first studies on this molecule²⁹ correctly reproduced the anomeric effect using the 4-31G basis set. A subsequent mapping of the two-dimensional

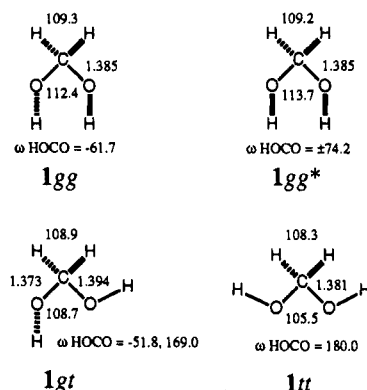


Figure 2. Selected geometrical data for the four stationary points of **1** calculated at the HF/6-31G** level. Isomers *1gg*, *1gg**, *1gt*, and *1tt* were optimized under constraints of C_2 , C_s , C_1 , and C_{2v} symmetry, respectively, and characterized by analytic frequency computation. Bond lengths are in Å, bond angles and dihedrals in deg.

potential surface for the coupled rotation of the two hydroxyl groups at the same level probed the effect more deeply.^{9b} Four stationary points were located, *1gg*, *1gg**, *1gt*, and *1tt*, where *g*, *g**, and *t* indicate HOCO dihedral angles of ca. 60°, -60°, and 180°, respectively. More recently, these isomers were examined at the HF/6-31G*, MP2/6-311++G**, MNDO, AM1, and PM3 levels by Woods et al.³⁰

Since most of this prior work employed constrained geometries, we performed full optimizations on all four stationary points. Selected geometrical details are presented in Figure 2. As previously observed, all are local minima except *1tt*, which has a single imaginary frequency of 157.3i. The MP2/6-31G** relative energies (kcal/mol) including zero point vibrational energy are *1gg*, 0.00; *1gg**, 3.09; *1gt*, 3.77; *1tt*, 8.13. Woods et al. optimized all geometric variables except for HOCO dihedrals, which they constrained to $\pm 60^\circ$ or 180° , and obtained relative energies (MP2/6-311++G** + ZPVE) of 0.00, 3.97, 3.41, and 7.51, respectively. Using AM1, they obtained relative heats of formation of 0.00, 3.56, 4.18, and 10.50, respectively; MNDO and PM3 did poorly, by comparison, at reproducing these energetics. Moreover, these authors noted an excellent agreement between the AM1 and MP2/6-31++G** geometrical parameters. The single exception was the OCO bond angle, which AM1 tended to underestimate by ca. 5°. However, AM1 did reproduce the experimentally^{1,6} and theoretically well-characterized angle widening observed for anomerically stabilized conformations: *1tt* with zero gauche dihedrals (i.e., zero opportunities for anomeric stabilization) has the narrowest OCO bond angle, followed by *1gt* with one gauche dihedral and than *1gg* and *1gg** each with two. The 1,5 eclipsing of hydroxyl protons in *1gg** accounts for the further slight angle widening exhibited by this isomer compared to *1gg*. The other hallmark of the anomeric effect, CO bond shortening for the donor oxygen and lengthening for the acceptor (Figure 2) is also well reproduced.^{30,31} This excellent performance prompted us to employ both AM1 and

(22) Dewar, M. J. S.; Zoebisch, E. G.; Healy, E. F.; Stewart, J. J. P. *J. Am. Chem. Soc.* **1985**, *107*, 3902.

(23) Francl, M. M.; Pietro, W. J.; Hehre, W. J.; Binkley, J. S.; Gordon, M. S.; DeFrees, D. J.; Pople, J. A. *J. Chem. Phys.* **1982**, *77*, 3654.

(24) (a) Møller, C.; Plesset, M. S. *Phys. Rev.* **1934**, *46*, 618. (b) Pople, J. A.; Binkley, J. S.; Seeger, R. *Int. J. Quant. Chem. Symp.* **1976**, *10*, 1.

(25) (a) Cramer, C. J.; Truhlar, D. G. *J. Am. Chem. Soc.* **1991**, *113*, 8305, 9901(E). (b) Cramer, C. J.; Truhlar, D. G. *Ibid.* **1991**, *113*, 8552, 9901(E).

(26) Frisch, M. J.; Head-Gordon, M.; Trucks, G. W.; Foresman, J. B.; Schlegel, H. B.; Raghavachari, K.; Robb, M.; Binkley, J. S.; Gonzalez, C.; DeFrees, D. J.; Fox, D. J.; Whiteside, R. A.; Seeger, R.; Melius, C. F.; Baker, J.; Martin, R. L.; Kahn, L. R.; Stewart, J. J. P.; Topiol, S.; Pople, J. A. *Gaussian 90 (Rev H)*, Gaussian Inc., Pittsburgh, PA.

(27) Cramer, C. J.; Lynch, G. C.; Truhlar, D. G. AMSOL-version 3.0. (Program no. 606 of the Quantum Chemistry Program Exchange, Indiana University, Bloomington, IN), *QCPE Bull.* **1992**, *12*, 62.

(28) Liotard, D. A.; Healy, E. F.; Ruiz, J. M.; Dewar, M. J. S. AMPAC-version 2.1 (program no. 506 of the Quantum Chemistry Program Exchange), *QCPE Bull.* **1989**, *10*, 86.

(29) Radom, L.; Hehre, W. J.; Pople, J. A. *J. Am. Chem. Soc.* **1971**, *93*, 289.

(30) Woods, R. J.; Szarek, W. A.; Smith, V. H., Jr. *J. Chem. Soc., Chem. Commun.* **1991**, 334.

(31) (a) In general, the HF/6-31G** calculations deliver bond lengths ca. 0.02 Å shorter for heavy atoms and 0.01 Å shorter for bonds to hydrogen, as expected, compared to either MP2/6-311++G** or AM1, where some form of correlation has been taken into consideration. Bond angles enjoy closer agreement. (b) Solvation effects for **1** and other neutral analogs have been explored computationally; see: Montagnani, R.; Tomasi, J. *Int. J. Quant. Chem.* **1991**, *39*, 851 and references cited therein.

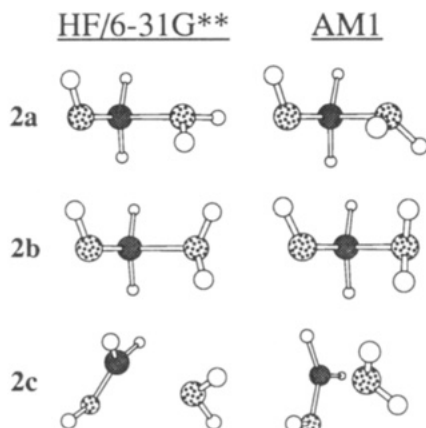


Figure 3. Structures for **2a–2c** calculated at the HF/6-31G** and AM1 levels. AM1-SM2 structures closely resemble AM1 structures and hence are not presented. Geometrical details may be found in Table I. All structures are local minima.

Table I. Selected Geometrical Data for 2a–2c at Various Levels of Computation^a

isomer	HF/6-31G**	AM1	AM1-SM2
2a			
rCO	1.301	1.353	1.380
rCO ⁺	1.659	1.564	1.479
∠OCO	105.1	98.0	101.4
ωHOCO ⁺	87.3	94.3	91.2
ωH ^a O ⁺ CO	178.7	134.6	144.8
ωH ^b O ⁺ CO	42.4	14.7	22.0
2b			
rCO	1.306	1.357	1.378
rCO ⁺	1.633	1.545	1.464
∠OCO	109.2	99.8	105.6
ωHOCO ⁺	93.3	104.7	92.6
ωH ^a O ⁺ CO	-79.6	-63.1	-54.5
ωH ^b O ⁺ CO	55.3	54.4	66.4
2c^b			
rCO	1.248	1.286	1.288
rCO ⁺	2.134	2.348	2.397
∠OCO	103.7	72.6	75.9
ωH ^a O ⁺ CO	-152.2		
ωH ^b O ⁺ CO	46.4		

^aAll structures were fully optimized. Bond lengths are in Å, bond angles and dihedrals in deg. ^bAt the semiempirical levels there is no appreciable carbon–oxygen interaction and the HOCO dihedrals are not particularly meaningful.

the solvation model built upon it, AM1-SM2, in our following studies as well.

(Hydroxymethyl)oxonium. Protonation of **1** delivers (hydroxymethyl)oxonium **2**, which exhibits two local minima. Each is characterized by a roughly 90° dihedral of the HOCO⁺ linkage. They differ primarily in the dihedral angle describing the lpO⁺CO geometry, where lp is the lone pair on the protonated oxygen. In **2a** it is between -70° and -105° and in **2b** it is ca. 180° depending on the calculational level. In addition to protonation of **1**, **2** may arise from addition of water to protonated formaldehyde, and conversely these are of course the expected products of acidic hydrolysis of **1**. We have thus additionally characterized **2c**, the ion dipole complex leading to **2**, as well as fully separated water and protonated formaldehyde. Figure 3 provides structural representations for **2a–2c**, while selected geometric and energetic details for the various levels of theory are provided in Tables I and II. The HF/6-31G** IR frequencies are provided in Table III.

To investigate anomeric stabilization into the σ*_{CO} orbital, we have analyzed the rotation coordinate about the unprotonated C–O bond. Since there are two local

Table II. Relative Energies (kcal/mol) for CH₅O₂ Isomers

isomer	MP2/6-31G** ^a	AM1	AM1-SM2	MP2 + ΔG _S ^{SM2b}	MP2 + ΔG _S ^{SM2} //HF ^c
2a^d	0.00	0.00	0.36	0.35	0.38
2b	0.27	0.26	0.00	0.00	0.00
2c	2.00	7.08	17.23	12.14	5.35
water + H ₂ COH ⁺	24.28	26.11	22.34	20.50	14.99

^aMP2/6-31G**//HF/6-31G** + ZPVE. ^bMP2/6-31G**//HF/6-31G** + ZPVE + AM1-SM2//AM1-SM2 - AM1//AM1. ^cMP2/6-31G**//HF/6-31G** + ZPVE + AM1-SM2//HF/6-31G** - AM1//HF/6-31G**. ^dAbsolute energies: MP2 + ZPVE = -190.66577 au, AM1 ΔH_f = 75.96 kcal/mol, AM1-SM2 ΔH_f + ΔG^o_S = -5.18 kcal/mol.

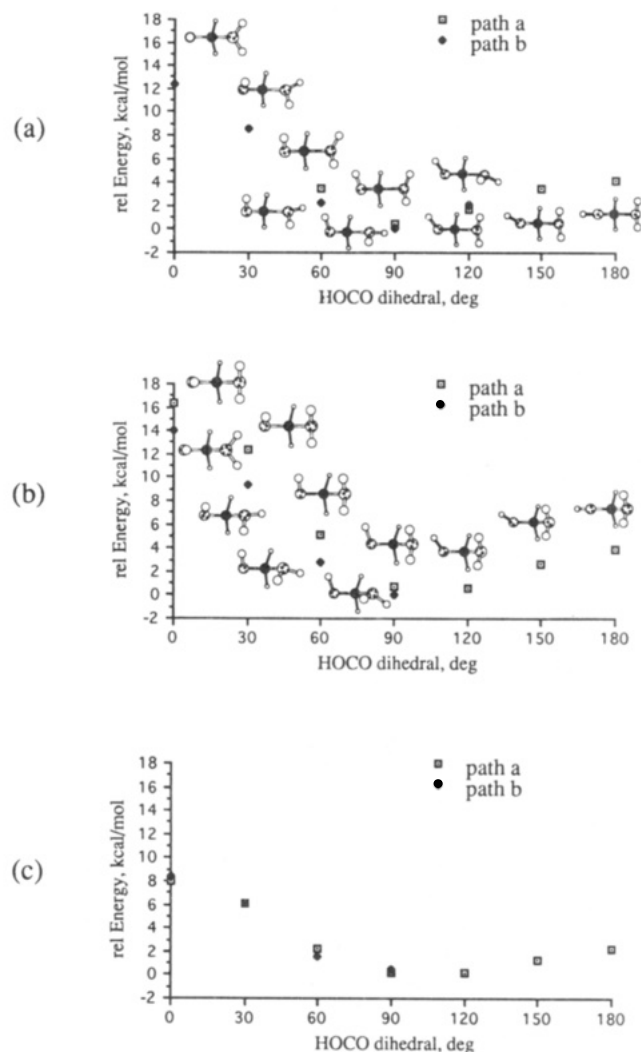


Figure 4. Energetics for hydroxyl group rotation in **2** (Table IV). The curves are symmetric for dihedral angles from 180° to 360°. Illustrations are placed as near as possible to every corresponding energy point; where there are two different structures with the same HOCO dihedral angle, the picture of the higher energy isomer appears above that of the lower energy isomer. The structures are similar enough at the AM1 and AM1-SM2 levels that they are omitted for the latter case. (a) HF/6-31G** level. (b) AM1 level. (c) AM1-SM2 level.

minima not related explicitly by this rotation, **2a** and **2b**, there are two rotational energy curves. At the ab initio level, these converge near HOCO⁺ dihedrals of both 45° and 135°. At the semiempirical levels, the curves only converge in the vicinity of an HOCO⁺ dihedral of 115°. In all cases, C_s structures with HOCO⁺ dihedrals of 0° and 180° were identified as true rotation barriers. The rota-

Table III. Frequencies (Unscaled) Calculated at the HF/6-31G** Level for 2a-2c

isomer	frequencies, ^a cm ⁻¹
2a	193.7, 265.7, 478.7, 613.1, 633.2, 924.4, 1142.3, 1282.3, 1405.4, 1494.3
2b	1515.0, 1691.1, 1772.4, 3321.1, 3438.0, 3878.9, 4094.7, 4105.7
2c	181.7, 271.2, 535.0, 566.9, 670.5, 864.3, 1165.3, 1345.2, 1381.0, 1501.2
	1505.9, 1675.9, 1798.2, 3320.9, 3436.9, 3980.5, 4092.0, 4118.5
	137.7, 167.8, 313.1, 329.2, 498.2, 617.4, 1014.1, 1198.4, 1339.8, 1499.1
	1556.1, 1757.2, 1785.5, 3349.2, 3496.2, 4037.4, 4087.6, 4195.0

^aFrequencies of intensity ≥ 100 km/mol are in italics.

Table IV. Energetics for Rotation about the Unprotonated C-O Bond in 2

ωHOCO^+	path ^a	HF/6-31G** ^b	AM1 ^b	AM1-SM2 ^c	HF + $\Delta G_{\text{S}}^{\text{SM2}}//\text{HF}^{\text{c,d}}$
0	a		16.36	8.05	
	b	12.37	14.07	8.42	4.75
30	a		12.43	6.04	
	b	8.55	9.40	6.08	3.64
60	a	3.53	5.11	2.24	1.55
	b	2.30	2.85	1.51	1.56
90	a	0.45	0.74	0.13	0.33
	b	0.02	0.04	0.45	0.33
120	a	1.70	0.67	0.24	-0.57
	b	2.12			-0.15
150	a	3.54	2.70	1.34	-0.97
180	a	4.12	3.84	2.18	-1.57

^aIndicates connectivity of rotational motion, see Figure 4.

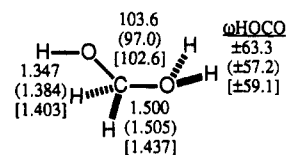
^bkcal/mol relative to 2a. ^ckcal/mol relative to 2b. ^dHF/6-31G** + AM1-SM2//HF/6-31G** - AM1/HF/6-31G**.

Table V. Relative Energies (kcal/mol) for CH₅O₂ Rotation Barriers^a

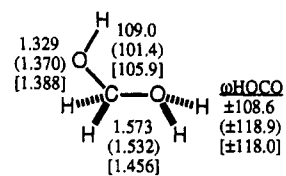
isomer	MP2/6-31G** ^b	AM1	AM1-SM2	MP2 + $\Delta G_{\text{S}}^{\text{SM2c}}$	MP2 + $\Delta G_{\text{S}}^{\text{SM2}}//\text{HF}^{\text{d}}$
2d	5.35 ^e	3.84	2.18	3.69	-0.34
2e	13.50 ^f	14.07	6.30	5.73	5.88
2f		16.36 ^g	8.05		

^aGas-phase energies are relative to 2a, energies including solvation are relative to 2b. ^bMP2/6-31G**//HF/6-31G** + ZPVE. ^cMP2/6-31G**//HF/6-31G** + ZPVE + AM1-SM2//AM1-SM2 - AM1//AM1. ^dMP2/6-31G**//HF/6-31G** + ZPVE + AM1-SM2//HF/6-31G** - AM1//HF/6-31G**. ^eImaginary frequency 252.1i. ^fImaginary frequency 689.4i. ^gImaginary frequency 752.7i.

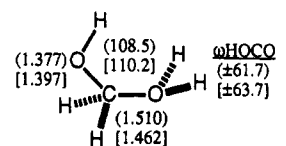
tional energetics are collected in Table IV and displayed for certain instances in Figure 4. Selected geometric details and energetics for the stationary points (transition states) 2d-2f may be found in Figure 5 and Table V, respectively. Isomer 2f is unstable to inversion through the protonated oxygen (delivering 2e) at the ab initio level, but is stationary on the semiempirical hypersurface. Tables VI and VII present, respectively, the two C-O bond lengths



2d



2e



2f

Figure 5. Selected geometrical data for hydroxyl group rotational barrier stationary points of 2 calculated at the HF/6-31G** (AM1) [AM1-SM2] level. All structures have C_s symmetry. Bond lengths are in Å, bond angles and dihedrals in deg.

and the Mulliken electronic populations on the OH and OH₂⁺ groups as a function of HOCO⁺ dihedral angle and theoretical model.

We have additionally investigated the rotational behavior of the protonated hydroxyl group in 2. Since the two local minima of 2 differ essentially as OH₂⁺ rotamers, there is only a single minimum energy curve on the hypersurface describing this motion (Figure 6). The energetics for rotation may be found in Table VIII. The low barrier between the two minima gives rise to a single rotational transition state, 2g, which has been characterized at the ab initio level. Because the corresponding local surface is so flat with respect to this rotation, no attempt

Table VI. Carbon-Oxygen Bond Lengths during Hydroxyl Group Rotation in 2

path ^a	ωHOCO^+ , deg	rCO, Å			rCO ⁺ , Å		
		HF/6-31G**	AM1	AM1-SM2	HF/6-31G**	AM1	AM1-SM2
a	0		1.377	1.397		1.510	1.462
	30		1.367	1.392		1.524	1.460
	60	1.307	1.355	1.385	1.634	1.547	1.464
	90	1.304	1.353	1.378	1.639	1.551	1.466
	120	1.323	1.363	1.392	1.569	1.536	1.463
	150	1.341	1.377	1.400	1.517	1.514	1.451
b	180	1.347	1.384	1.403	1.500	1.505	1.437
	0	1.329	1.370	1.388	1.573	1.532	1.456
	30	1.320	1.361	1.382	1.595	1.543	1.464
	60	1.304	1.351	1.378	1.648	1.566	1.476
	90	1.302	1.352	1.376	1.654	1.566	1.478
	120	1.323			1.578		

^aSee Figure 4.

Table VII. Total Mulliken Population for the OH and OH₂⁺ Groups During Hydroxyl Group Rotation in 2

path ^a	ω HOCO ⁺ , deg	q(OH), au			q(OH ₂ ⁺), au		
		HF/6-31G**	AM1	AM1-SM2	HF/6-31G**	AM1	AM1-SM2
a	0		-0.037	-0.108		0.500	0.665
	30		-0.019	-0.099		0.477	0.656
	60	-0.120	0.007	-0.081	0.282	0.451	0.647
	90	-0.136	0.011	-0.072	0.429	0.457	0.649
	120	-0.162	-0.008	-0.084	0.403	0.495	0.679
	150	-0.172	-0.040	-0.102	0.410	0.546	0.716
	180	-0.245	-0.060	-0.111	0.541	0.571	0.751
b	0	-0.250	0.009	-0.097	0.525	0.482	0.658
	30	-0.147	0.023	-0.068	0.453	0.460	0.652
	60	-0.112	0.043	-0.053	0.283	0.432	0.628
	90	-0.170	0.036	-0.047	0.412	0.441	0.626
	120	-0.162			0.361		

^a See Figure 4.

Table VIII. Energetics for Rotation about the Protonated C-O Bond in 2

ω lpO ⁺ CO	HF/6-31G** ^a	AM1 ^a	AM1-SM2 ^b	HF + ΔG_s^{SM2} // HF ^{b,c}
0		4.58	4.47	
15		4.98		
30		5.02	4.59	
45		4.75		
60		4.25	3.81	
75		3.60		
90		2.86	3.44	
105		2.10		
120		1.41	2.48	
135		0.84		
150	0.58	0.46	1.54	0.69
165	0.43	0.28		0.16
180	0.51	0.26	0.21	0.10
195	0.80	0.29		0.69
210	1.12	0.28	1.34	1.66
225	1.28	0.19		2.02
240	1.13	0.06	1.16	1.78
255	0.73	0.00		1.27
270	0.28	0.14	0.59	0.75
285	0.02	0.55		0.35
300	0.06	1.19	1.33	0.92
315		2.04		
330		2.96	2.70	
345		3.86		

^a kcal/mol relative to 2a. ^b kcal/mol relative to 2b. ^c HF/6-31G** + AM1-SM2//HF/6-31G** - AM1//HF/6-31G**.Table IX. Relative Energies (kcal/mol) for Additional CH₂O₂ Transition States^a

isomer	MP2/6-31G** ^b	MP2 + ΔG_s^{SM2} // HF ^c
2g	0.99 ^d	1.75
2h	0.52 ^e	4.78
2i	0.17 ^f	4.12

^a Gas-phase energies are relative to 2a, energies including solvation are relative to 2b. ^b MP2/6-31G**//HF/6-31G** + ZPVE. ^c MP2/6-31G**//HF/6-31G** + ZPVE + AM1-SM2//HF/6-31G** - AM1//HF/6-31G**. ^d Imaginary frequency 203.3i. ^e Imaginary frequency 193.1i. ^f Imaginary frequency 169.1i.

was made to explicitly locate this transition state at the semiempirical levels.

Interestingly, at the ab initio level, (hydroxymethyl)oxonium is stable to dissociation to the ion-dipole complex 2c only for lpO⁺CO dihedral angles between ca. 150° and 330°. The two transition states corresponding to bond breakage, 2h and 2i, have also been located and characterized. Geometric details for these last three stationary points may be found in Figure 7 and energetic information in Table IX.**(Hydroxymethyl)ammonium.** Because of the availability of experimental data relating to the reverse anomericTable X. Relative Energies (kcal/mol) for CH₂NO Isomers

isomer	MP2/6-31G** ^a	AM1	AM1-SM2	MP2 + ΔG_s^{SM2b}	MP2 + ΔG_s^{SM2} // HF ^c
3a ^d	0.00	0.00	0.00	0.98	0.78
3b	0.17	2.38	1.23	0.00	0.00
3c	11.15	9.18	5.20	8.15	8.49
3d	-0.02 ^e				0.62

^a MP2/6-31G**//HF/6-31G** + ZPVE. ^b MP2/6-31G**//HF/6-31G** + ZPVE + AM1-SM2//AM1-SM2 - AM1//AM1. ^c MP2/6-31G**//HF/6-31G** + ZPVE + AM1-SM2//HF/6-31G** - AM1//HF/6-31G**. ^d Absolute energies: MP2 + ZPVE = -170.86396 au, AM1 ΔH_f = 102.03 kcal/mol, AM1-SM2 ΔH_f + ΔG_s = 25.95 kcal/mol. ^e ZPVE causes 3d to drop below 3a and 3b in energy; given the uncertainties in low- to mid-frequency modes, this should hardly be regarded as definitive.

Table XI. Relative Energies (kcal/mol) for Isomers of 4 and 5

isomer	MP2/6-31G** ^a	AM1	AM1-SM2	MP2 + ΔG_s^{SM2b}	MP2 + ΔG_s^{SM2} // HF ^c
4eq ^d	0.00	0.87	0.00	0.00	0.00
4ax	1.01	0.00	1.19	3.07	3.25
5eq ^e	0.00	3.30	1.17	0.00	0.00
5ax	2.24	0.00	0.00	4.37	5.51

^a MP2/6-31G**//HF/6-31G** + ZPVE. ^b MP2/6-31G**//HF/6-31G** + ZPVE + AM1-SM2//AM1-SM2 - AM1//AM1. ^c MP2/6-31G**//HF/6-31G** + ZPVE + AM1-SM2//HF/6-31G** - AM1//HF/6-31G*. ^d Absolute energies: MP2 + ZPVE = -290.35566 au, AM1 ΔH_f = 115.12 kcal/mol, AM1-SM2 ΔH_f + ΔG_s = 55.27 kcal/mol. ^e Absolute energies: MP2 + ZPVE = -326.23138 au, AM1 ΔH_f = 90.51 kcal/mol, AM1-SM2 ΔH_f + ΔG_s = 28.30 kcal/mol.effect for protonated amine substituents,^{17,32} we have also investigated (hydroxymethyl)ammonium, 3. The lack of a lone pair on the ammonium group simplifies the hypersurface considerably by comparison to 2; rather than exploring the complete rotation coordinate about the C-O bond, we have simply characterized the various stationary points along it. At the ab initio level, there are two local minima, one in which the HOCN dihedral is 115.1°, 3a, and one in which it is trans, 3b. By contrast, the latter conformer, of C_s symmetry, is predicted at the semiempirical level to be a transition state (AM1 frequency 244.2i). Both levels of theory predict the C_s isomer 3c, in which the OH bond eclipses the CN, to be a transition state (ab initio frequency 641.2i). Finally, the transition state separating 3a and 3b at the ab initio level has also been located (3d, ab initio frequency 176.4i). Structural details are collected in Figure 8, energetics in Table X.

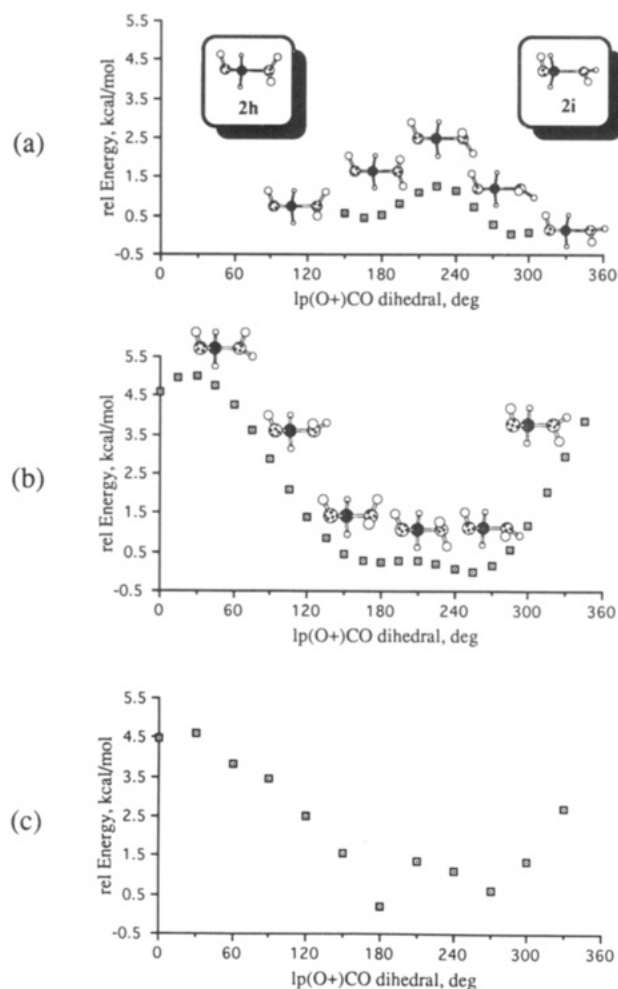
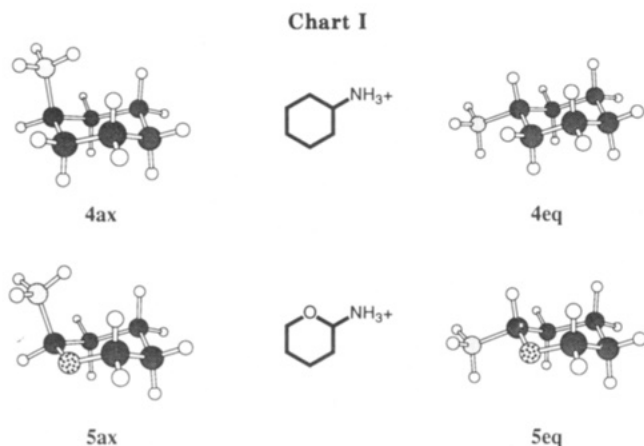


Figure 6. Energetics for rotation of the protonated hydroxyl group in **2** (Table VIII). The oxygen lone pair is defined to lie in the plane bisecting the two protons of the oxonium group for dihedral angle calculation purposes. At the ab initio level, the curve endpoints are in regions where spontaneous CO bond breakage occurs, with the appropriate transition states shown. The structures are similar enough at the AM1 and AM1-SM2 levels that they are omitted for the latter case. (a) HF/6-31G** level (illustrations are 150, 195, 225, 255, 300). (b) AM1 level (illustrations are 30, 90, 150, 210, 270, 330). (c) AM1-SM2 level.



Six-Membered Rings. To complete our survey, we focused on two molecules of more relevance to sugar series. In particular, we compared the energetics for axial and equatorial substitution in cyclohexylammonium, **4**, and 2-tetrahydropyranosylammonium, **5** (Chart I). The former, of course, has no potential for exhibiting any kind of anomeric effect, and indeed **4eq** is favored over **4ax** by 1.01

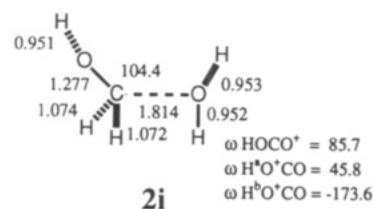
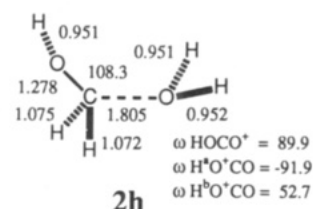
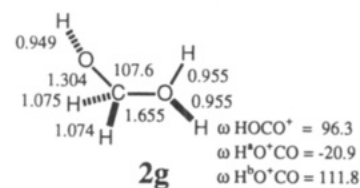


Figure 7. Selected geometrical data for **2g–2i** calculated at the HF/6-31G** level. All structures are transition states of C_1 symmetry. Bond lengths are in Å, bond angles and dihedrals in deg.

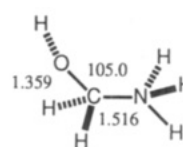
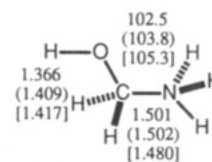
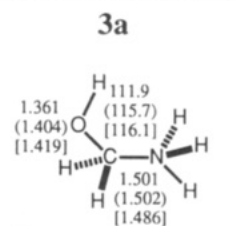
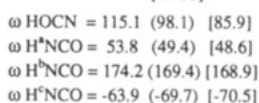
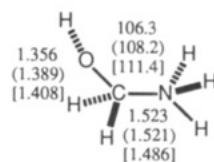


Figure 8. Selected geometrical data for **3a–3d** calculated at the HF/6-31G** (AM1) [AM1-SM2] level. Structures **3b** and **3c** have C_s symmetry while **3a** and **3d** are C_1 . Bond lengths are in Å, bond angles and dihedrals in deg.

kcal/mol. On going to **5**, in seeming contravention of the anomeric effect, this preference increases to 2.24 kcal/mol.

For these two systems one observes, for the first time, a very poor agreement between AM1 and the ab initio level. The fault appears to lie with the semiempirical model, given that it predicts alicyclic cyclohexylammonium to prefer an axial substitution pattern over an equatorial. Here, then, solvation effects are better added to ab initio energy differences than to those from AM1 (vide infra).

Discussion

As mentioned above, all calculations on dihydroxymethane, including our own, reproduce the gross structural and energetic features of the anomeric effect, viz., stabilization of structures permitting $n_{\text{O}} \rightarrow \sigma_{\text{CO}}^*$ delocalization

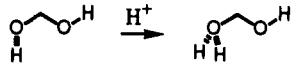
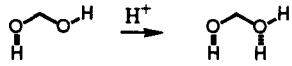
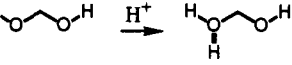
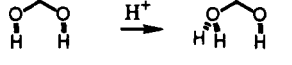
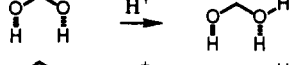
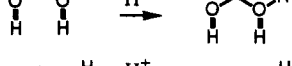
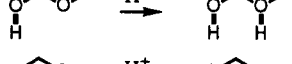
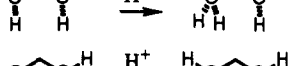
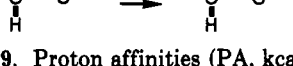
Reaction	PA	§	‡
	186.2	Yes	No
	185.7	Yes	Yes
	185.0	Yes	No
	185.0	Yes	Yes
	181.8	No	Yes
	181.8	No	Yes
	181.4	No	Yes
	180.6	No	Yes
	180.3	No	No

Figure 9. Proton affinities (PA, kcal/mol) of Woods, Szarek, and Smith (taken from ref 30) at MP2/6-311++G** level. Structures were optimized employing ideal HOCO dihedral angles, i.e., $\pm 60^\circ$ or 180° . §: Protonation occurs at one of two 1,5-eclipsing lone pairs, ‡: the reaction product permits $n_O \rightarrow \sigma^*_{CO^+}$ delocalization.

with concomitant shortening of the $C-O_{\text{donor}}$ bond, lengthening of the $C-O_{\text{acceptor}}$ bond, and widening of the OCO bond angle. The calculations of Woods and co-workers,³⁰ employing idealized HOCO dihedrals, are no exception. These authors extended these calculations to (hydroxymethyl)oxonium, again with idealized HOCO dihedrals. While these constrained optimizations led them to some unfortunate conclusions regarding the reverse anomeric effect (vide infra), they allow an interesting test of Deslongchamp's hypothesis^{1e} that oxygen atoms involved as part of the acceptor σ^*_{CO} orbital should be more basic than otherwise. The results of Woods et al. are presented in Figure 9, where it is seen that the nine possible protonations (given the constrained dihedrals) separate into two groups. Each member of the first group of four has a ca. 4 kcal/mol higher proton affinity than those from the second group of five. Interestingly, four of the six cases where protonation occurs at the anomeric acceptor oxygen atom are found in the *low* affinity group. Perhaps not surprisingly, it appears that hyperconjugative contributions to basicity are far outweighed by simpler electrostatic considerations, namely that protonation is favored at a lone pair which is one of two which are 1,5-eclipsed. It is this distinction which separates the high-affinity group from the low. Hyperconjugative contributions to basicity appear to be too subtle in this instance to be readily separated from the other effects, such as sterics, which further modify the predominant electrostatics.

Turning to a more detailed consideration of the anomeric effect in (hydroxymethyl)oxonium, inspection of Figure 3 illustrates that the two local minima, **2a** and **2b**, do indeed adopt geometries permitting $n_O \rightarrow \sigma^*_{CO^+}$ delocalization. However, because of unfavorable electrostatic interactions between the hydroxyl and oxonium protons in this positively charged species, the preferred HOCO⁺ dihedral is generally near 90° as opposed to the ideal gauche dihedral of 60° . Indeed, because of this repulsive

interaction, for both local minima the energy rises quite steeply as the HOCO⁺ dihedral goes from 90° to 0° —so much so that in each case the ideal gauche isomer is slightly higher in energy than the ideal trans isomer, where ωHOCO^+ is 180° . By sampling only these ideal dihedrals, Woods et al. were led to conclude that (hydroxymethyl)oxonium demonstrated a phenomenological reverse anomeric effect. This is, however, evidently not the case.

Further evidence in this regard is provided by the data in Table VI. For each methodology, there is a smooth increase in the r_{CO^+} bond length, with a concomitant decrease in the r_{CO} bond length, on going from HOCO⁺ dihedrals of 0° or 180° (minimal delocalization overlap) to 90° (maximal overlap). In the ab initio case, the lengthening of the $C-O^+$ bond is quite dramatic, going from 1.500 to 1.639 Å! The minimal basis semiempirical methods are somewhat biased against such stretched bonds, but nevertheless show significant lengthening. Still better agreement on r_{CO} bond shortening is found between the disparate methods. Finally, inspection of the group charges for the OH and OH_2^+ groups as a function of HOCO⁺ dihedral is instructive. Table VII shows a significant shift of electrons from the donor hydroxyl to the oxonium acceptor group on going from minimal overlap to maximal, i.e., 180° to 90° . Again the effect is more profound at the ab initio level, but the sensitivity of Mulliken charges to calculational level is well established, and no quantitative meaning should be inferred.

While it is evident that hyperconjugation plays a large role in the C–O rotation coordinate, it is equally apparent that it plays little if any role in that for C–O⁺. Focusing for the moment on Figure 6b, the shape of the rotational curve suggests that it is dipole effects which dominate the energetics,^{9b,33} and indeed, there is a direct correspondence between increasing dipole moment and increasing energy. Thus, for the rotation barrier near $\omega\text{lpO}^+\text{CO} = 30^\circ$, the dipole moment reaches its maximum of 4.6 D. In the broad, flat region between $\omega\text{lpO}^+\text{CO}$ values of 150° and 270° , the dipole varies from 1.9 to 2.9 D. While the minimum occurs near $\omega\text{lpO}^+\text{CO} = 210^\circ$, eclipsing of the oxonium and methylene protons in this conformation causes it to rise somewhat in energy, becoming a low-energy barrier separating **2a** and **2b**. In the ab initio case, the trend in dipole moment is identical, although C–O⁺ bond dissociation is predicted when the dipole moment exceeds 3.2 D, which occurs both at ca. 150° and 300° lpO^+CO dihedral angles. The steric contribution to the rotational saddle point **2g** is also about 0.7 kcal/mol higher. In neither the ab initio nor the semiempirical cases is there any apparent geometrical or energetic evidence of hyperconjugative delocalization of the oxonium lone pair into the σ^*_{CO} orbital.

With respect to the issue of dissociation, the semiempirical rotation curve may well be more accurate than the ab initio. In the absence of accounting for correlation at the MP2 level, the ion–dipole complex **2c** is the global minimum on the local ab initio hypersurface, with **2a** and **2b** lying 0.36 and 0.79 kcal/mol higher in energy, respectively. Thus, at the HF level alone, the barrier to dissociation is probably well underestimated. However, characterization of the rotation coordinate at the correlated level is prohibitively expensive.

In (hydroxymethyl)ammonium we have a model which more closely relates to the ammonium species which initially gave rise to the categorization of a reverse anomeric effect. And indeed, there are significant differences be-

(33) Radom, L.; Hehre, W. J.; Pople, J. A. *J. Am. Chem. Soc.* **1972**, *94*, 2371.

tween this compound and 2. Although 3a, the minimum energy isomer in the gas phase, continues to adopt an anomalously stabilized geometry, it is only slightly stabilized over 3b, the transoid isomer. The smaller degree of stabilization is consistent with the much smaller lengthening of the C-N and shortening of the C-O bond lengths on going from 3b to 3a compared to the analogous C-O⁺ and C-O bond lengths in 2. It is also consistent with the similar sizable degradation in $n_O \rightarrow \sigma^*_{CN}$ anomeric delocalization in aminomethanol by comparison to the $n_O \rightarrow \sigma^*_{CO}$ process in dihydroxymethane.^{14,34}

Thus, the smaller ab initio dipole moment of 3b (3.6 D) compared to 3a (4.3 D), together with the weakened anomeric effect, contributes to a significant lowering of the gauche-trans energy difference for 3 relative to 2. At the semiempirical level, it merely reduces what is still a rotation barrier to a relative energy of 2.4 kcal/mol. At the ab initio level, again the steric repulsion of eclipsing vicinal protons is higher, and this suffices to make 3b a very shallow local minimum separated from 3a by an extremely low barrier, 3d. The eclipsed conformer, 3c, continues to represent a sizable barrier to C-O rotation at all levels.

Finally, in 4 and 5 we include the steric effects of the six-membered rings. Compound 4 was calculated primarily to provide some insight into the steric component of the axial-equatorial equilibrium in 5. In the absence of any opportunity for an anomeric effect, it is unsurprising that the C-N bond lengths are nearly identical in 4eq and 4ax at 1.528 and 1.534 Å, respectively; the CCN bond angles are similarly close at 108.9° and 108.8°, respectively. Moreover, the magnitude of the ab initio equatorial preference is in the range of what might be expected based on substituted amines.³⁵

By applying Franck's suggested conversion factor for relating steric effects in cyclohexanes to tetrahydropyrans,³⁶ and assuming the observed equatorial preference in 4 is indeed entirely steric, we would expect a 1.55 kcal/mol steric preference favoring 5eq. The observed preference of 2.24 kcal/mol indicates additional factors at work which favor the equatorial conformer. However, this is not to say that there is no anomeric stabilization in 5ax. Quite the contrary, on going from 5eq to 5ax the CN bond length goes from 1.513 to 1.561 Å and the OCN bond angle expands from 101.9° to 106.9°, both indicative of anomeric delocalization.

As suggested by Lemieux and Morgan,¹⁷ it is almost certainly a consideration of the local dipoles for the two heteroatomic fragments of the molecule which gives rise to this effect. The situation is similar to that illustrated in Figure 1a, except that the dipole for the ammonium substituent is reversed by comparison to the ether, thereby favoring the equatorial isomer. Ironically, it is likely the discredited explanation for the anomeric effect which best explains the dominant electronics of the reverse anomeric effect! Thus, geometric analysis indicates that anomeric stabilization into the accepting σ^*_{CN} orbital does occur in 5ax, but it is overwhelmed by steric and local dipole effects which favor 5eq. As a result, the equatorial 2-amino-tetrahydropyran isomer is expected to be more basic than the axial, especially since the normal anomeric effect

stabilizes the axial (neutral) amine.

Considering this system as a model for hydrolysis of polysaccharides, however, does not necessarily lead to a clear picture of axial vs equatorial basicity. At the ab initio level, a comparison of the energy difference between 2a (or 2b) and 2d with that between 3a and 3b indicates anomeric delocalization to be about 5 kcal/mol more stabilizing in the former case. However, at the semiempirical level, the additional stabilization amounts to only about 1.5 kcal/mol. Given the 2.24 kcal/mol preference for 5eq over 5ax, it is clearly not easy to predict the relative basicities of equatorial and axial 2-hydroxytetrahydropyran. However, assessing the effects of aqueous solvation may provide a more definitive analysis.

Solvation. Aqueous solvation has a number of significant effects on both the energetics and the structures for 2. The largest geometric effect is illustrated in Tables I and VI, where the CO⁺ bond lengths contract by up to 0.085 Å on going from the AM1 to the AM1-SM2 model. The CO bond is simultaneously found to be up to 0.03 Å longer. Table VII indicates this to be at least partly due to the decreased tendency for electronic charge to flow from the hydroxyl group to the oxonium group, which is better able to accommodate positive charge while solvated. Since the mechanism of that charge flow is in large part hyperconjugative, i.e., the anomeric effect, attenuating it reduces its geometrical consequences.

Energetically, solvation significantly increases the relative energies of the ion-dipole complex 2c and the dissociative transition states 2h and 2i. This is exactly as expected given the dissipated nature of the unit charge in these structures relative to 2a and 2b and suggests that, as expected, 2 will be more stable in solution than in the gas phase. Conversely, because of the greater concentration of charge in protonated formaldehyde, solvation considerably lowers the energy of the separated dissociation products. It is the same concentration of charge, in this case resulting from bringing the hydroxyl and oxonium protons into close proximity, which gives rise to the sizable stabilizations for 2e and 2f relative to 2a and 2b. Finally, 2d is stabilized over 2a and 2b because of the decreased internal dielectric shielding in this most extended conformation of the molecule: it is more accessible to the solvent.²⁷ Indeed, employing the technique of calculating AM1-SM2 solvation free energies at the ab initio geometries, 2d appears to be the lowest energy point on the rotational curve (Table IV). However, this is the least desirable of the three approaches described in the Methods section for assessing solvation energy because of the nonstationary (at the AM1-SM2 level) nature of the structures. It suffices to say that aqueous solvation will cause the rotational potential through 2d connecting the two enantiomeric conformers of 2a or 2b to be relatively flat.

For 3, the situation is much the same except that the smaller energy gap separating the gauche and anti isomers causes the effects of solvation to be more noticeable. Thus, if one adds the semiempirical solvation energies to the ab initio gas-phase energies, one finds the anti isomer 3b to now be favored over the gauche isomer 3a.³⁸ The entirely semiempirical result maintains the gas-phase ordering, but the relative difference between the two methods amounts to only 2.2 kcal/mol, again suggesting a very flat rotational hypersurface between the two enantiomeric gauche conformers.

Finally, 4 and 5 are interesting inasmuch as solvation favors the equatorial (trans) isomer over the axial (gauche) in each case by about 2 kcal/mol. Because of the im-

(34) (a) Schafer, L.; Van Alsenoy, C.; Williams, J. O.; Scarsdale, J. N.; Geise, H. J. *THEOCHEM* 1981, 76, 349. (b) Senderowitz, H.; Aped, P.; Fuchs, B. *Helv. Chim. Acta* 1990, 73, 2113. (c) Fernández, B.; Ríos, M. A.; Carballeira, L. *J. Comput. Chem.* 1991, 12, 78. (d) For methoxymethylammonium, see: Krol, M. C.; Huige, C. J. M.; Altona, C. *Ibid* 1990, 11, 765.

(35) Booth, H.; Josefowicz, M. L. *J. Chem. Soc., Perkin Trans. 2* 1976, 895.

(36) Franck, R. W. *Tetrahedron* 1983, 39, 3251.

Table XII. Separation of Free Energy of Solvation Terms (kcal/mol) for 4 and 5^a

isomer	ΔG_{ENP}	G°_{CDS}	$\Delta G^{\circ}_{\text{S}}$
4eq	-58.09	-1.76	-59.85
4ax	-56.42	-1.38	-57.80
5eq	-59.43	-2.78	-62.21
5ax	-57.36	-2.72	-60.08

^a AM1-SM2//AM1-SM2.

portance of these systems, it is worthwhile to break down the solvation free energy, $\Delta G^{\circ}_{\text{S}}$, into the two components ΔG_{ENP} and G°_{CDS} (Table XII).^{21,25a,37} The first accounts for electronic polarization of the solute by the solvent and electric polarization of the solvent by the solute and essentially derives from the entire solvent cosphere. The latter term, on the other hand, is associated almost entirely with the first solvation shell and accounts for, inter alia, cavitation, dispersion effects, and disrupted local water structure.

As expected given that these substrates bear a full positive charge, the solvation free energies are heavily dominated by the ΔG_{ENP} term. In 4, this term is larger for the equatorial isomer by 1.67 kcal/mol, while in 5 the difference is 2.07 kcal/mol.³⁹ There are essentially two major influences conformation can have on ΔG_{ENP} . The first is to significantly change the distribution of charge in space as represented by atom-centered monopoles. However, since in 4 the dominant charge in space is almost entirely localized in the close vicinity of the ammonium group, this plays little role. Rather, it is the second influence, bulk shielding of the charge from the surrounding dielectric, which accounts for the vast majority of the 1.67 kcal/mol. This is consistent with the 0.38 kcal/mol smaller G°_{CDS} term observed for 4ax; this latter term is a function of solvent accessible surface area and thus relates intuitively with dielectric shielding.

This suggests that the change in ΔG_{ENP} on going from 5eq to 5ax, by virtue of being similar in magnitude, is also largely a function of dielectric shielding. In this instance, $\Delta G^{\circ}_{\text{CDS}}$ is less helpful since the destabilizing decrease in solvent accessible surface area for the ammonium group is balanced by a stabilizing increase for the ether, resulting in a net increase in G°_{CDS} of only 0.06 kcal/mol.

In general then, it appears that dielectric shielding of axial groups from favorable solvation will tend to decrease their relative basicity by comparison to equatorial groups. So, in spite of the anomeric delocalization that occurs for charged axial groups in the tetrahydropyran system, steric

effects, dipole-dipole effects, and solvation effects all drive the axial-equatorial equilibrium in the opposite direction. It is noteworthy that in simple, uncharged, 2-substituted tetrahydropyrans, the ΔG_{ENP} solvation terms will tend to be roughly an order of magnitude smaller, as will the differences between them. Thus, the influence of solvation on such systems should not be quite so profound, albeit still important.

Conclusion

In (hydroxymethyl)oxonium the preference for the gauche isomer over the trans (which is a rotation barrier) is greater than for dihydroxymethane. Noting this, and additionally noting telltale geometric and electronic evidence, it is clear that anomeric delocalization remains operative in this molecule. While the σ^*_{CN} orbital in (hydroxymethyl)ammonium appears to be a somewhat weaker acceptor than the $\sigma^*_{\text{CO}^+}$ in (hydroxymethyl)oxonium, as judged by the smaller preference for the gauche isomer over the trans (now a local minimum ab initio), nevertheless there is still a noticeable anomeric effect. This effect is conserved upon incorporation into the 2-tetrahydropyranosylammonium system; however, it is there opposed by sterics, by local dipole-dipole effects, and by aqueous solvation. The combination of these latter effects is sufficient to drive the equilibrium heavily to the (trans) equatorial isomer, i.e., a reverse anomeric situation.

Aqueous solvation in the acyclic systems tends to slightly decrease the anomeric effect because in the extended trans conformation there is better accessibility of the solute to the solvent and somewhat more polarization of charge. In the tetrahydropyran system, dielectric shielding of the ammonium group by the ring system disfavors the axial isomer by ca. 2 kcal/mol compared to the equatorial. However, this effect is expected to decrease by roughly 1 order of magnitude in uncharged systems.

These results suggest that in the absence of other substituent effects, equatorially disposed amines, and by extension ethers, at the anomeric position in sugars will be more basic (in a thermodynamic sense) than those disposed axially. Moreover, protonation will occur preferentially at lone pairs which are eclipsed in a 1,5-fashion with another lone pair on the ring oxygen. This has some interesting impact on the hydrolysis/opening of asymmetric acetals.⁴⁰ We will continue to develop these themes in future work.

Acknowledgment. This work was supported in part by the Minnesota Supercomputer Institute.

Supplementary Material Available: Ab initio energies and Z-matrices for all stationary points for 2-5 (4 pages). This material is contained in many libraries on microfiche, immediately follows this article in the microfilm version of the journal, and can be ordered from the ACS; see any current masthead page for ordering information.

(37) For a detailed discussion of conformational issues as they affect the SMx models, see: Cramer, C. J.; Truhlar, D. G. *J. Comput.-Aid. Mol. Des.*, in press.

(38) A similar situation holds for dopamine, Urban, J. J.; Cramer, C. J.; Famini, G. R. *J. Am. Chem. Soc.* 1992, 114, 8226.

(39) It is worth noting that the ΔG_{ENP} term is an analytic expression relying on solvent dielectric and parameters which describe atomic radius as a function of charge. These latter terms are largely independent of solvent. Thus, extension of these results to nonaqueous solvents is relatively straightforward and proportional to $(1 - 1/\epsilon)$ where ϵ is the solvent dielectric.

(40) Denmark, S. E.; Almstead, N. G. *J. Am. Chem. Soc.* 1991, 113, 8089 and references found therein.